

Search for pseudoscalar bosons decaying into e^+e^- pairs in the NA64 experiment at the CERN SPS

Yu. M. Andreev,⁶ D. Banerjee,⁴ J. Bernhard,⁴ V. E. Burtsev,² N. Charitonidis,⁴ A. G. Chumakov,^{12,13} D. Cooke,⁵ P. Crivelli,¹⁵ E. Depero,¹⁵ A. V. Dermenev,⁶ S. V. Donskov,¹⁰ R. R. Dusaev,¹² T. Enik,² A. Feshchenko,² V. N. Frolov,² A. Gardikiotis,⁹ S. G. Gerassimov,^{3,7} S. N. Gninenko,⁶ M. Hösgen,¹ M. Jeckel,⁴ V. A. Kachanov,¹⁰ A. E. Karneyeu,⁶ G. Kekelidze,² B. Ketzer,¹ D. V. Kirpichnikov,⁶ M. M. Kirsanov,⁶ V. N. Kolosov,¹⁰ I. V. Konorov,^{3,7} S. G. Kovalenko,^{11,16} V. A. Kramarenko,^{2,8} L. V. Kravchuk,⁶ N. V. Krasnikov,^{2,6} S. V. Kuleshov,^{11,16} V. E. Lyubovitskij,^{12-14,16} V. Lysan,² V. A. Matveev,² Yu. V. Mikhailov,¹⁰ L. Molina Bueno,^{15,17} D. V. Peshekhonov,² V. A. Polyakov,¹⁰ B. Radics,¹⁵ R. Rojas,¹⁴ A. Rubbia,¹⁵ V. D. Samoylenko,¹⁰ H. Sieber,¹⁵ D. Shchukin,⁷ V. O. Tikhomirov,⁷ I. Tlisova,⁶ A. N. Toropin,⁶ A. Yu. Trifonov,^{12,13} B. I. Vasilishin,¹² G. Vasquez Arenas,¹⁴ P. V. Volkov,^{2,8} V. Yu. Volkov,⁸ and P. Ulloa¹¹

(The NA64 Collaboration)

¹Universität Bonn, Helmholtz-Institut für Strahlen-und Kernphysik, 53115 Bonn, Germany

²Joint Institute for Nuclear Research, 141980 Dubna, Russia

³Technische Universität München, Physik Department, 85748 Garching, Germany

⁴CERN, European Organization for Nuclear Research, CH-1211 Geneva, Switzerland

⁵UCL Department of Physics and Astronomy, University College London, Gower St., London WC1E 6BT, United Kingdom

⁶Institute for Nuclear Research, 117312 Moscow, Russia

⁷P.N. Lebedev Physical Institute of the Russian Academy of Sciences, 119 991 Moscow, Russia

⁸Skobeltsyn Institute of Nuclear Physics, Lomonosov Moscow State University, 119991 Moscow, Russia

⁹Physics Department, University of Patras, 265 04 Patras, Greece

¹⁰State Scientific Center of the Russian Federation Institute for High Energy Physics of National Research Center ‘Kurchatov Institute’ (IHEP), 142281 Protvino, Russia

¹¹Departamento de Ciencias Físicas, Universidad Andres Bello, Sazié 2212, Piso 7, Santiago, Chile

¹²Tomsk Polytechnic University, 634050 Tomsk, Russia

¹³Tomsk State Pedagogical University, 634061 Tomsk, Russia

¹⁴Universidad Técnica Federico Santa María, Centro Científica y Tecnológica de Valparaíso-CCTVal, 2390123 Valparaíso, Chile

¹⁵ETH Zürich, Institute for Particle Physics and Astrophysics, CH-8093 Zürich, Switzerland

¹⁶Millennium Institute for Subatomic Physics at the High-Energy Frontier (SAPHIR) of ANID, Fernández Concha 700, Santiago, Chile

¹⁷Instituto de Física Corpuscular (CSIC/UV), Carrer del Catedrtic Jos Beltrn Martinez, 2, 46980 Paterna, Valencia



(Received 14 May 2021; accepted 19 November 2021; published 15 December 2021)

We report the results of a search for a light pseudoscalar particle a that couples to electrons and decays to e^+e^- performed using the high-energy CERN SPS H4 electron beam. If such light pseudoscalar exists, it could explain the ATOMKI anomaly (an excess of e^+e^- pairs in the nuclear transitions of ^8Be and ^4He nuclei at the invariant mass $\simeq 17$ MeV observed by the experiment at the 5 MV Van de Graaff accelerator at ATOMKI, Hungary). We used the NA64 data collected in the “visible mode” configuration with a total statistics corresponding to 8.4×10^{10} electrons on target (EOT) in 2017 and 2018. In order to increase sensitivity to small coupling parameter ϵ we also used the data collected in 2016–2018 in the “invisible mode” configuration of NA64 with a total statistics corresponding to 2.84×10^{11} EOT. The background and efficiency estimates for these two configurations were retained from our previous analyses searching for light vector bosons and axionlike particles (ALP) (the latter were assumed to couple predominantly to γ). In this

work we recalculate the signal yields, which are different due to different cross section and lifetime of a pseudoscalar particle a , and perform a new statistical analysis. As a result, the region of the two dimensional parameter space $m_a - \epsilon$ in the mass range from 1 to 17.1 MeV is excluded. At the mass of the central value of the ATOMKI anomaly (the first result obtained on the beryllium nucleus, 16.7 MeV) the values of ϵ in the range $2.1 \times 10^{-4} < \epsilon < 3.2 \times 10^{-4}$ are excluded.

DOI: [10.1103/PhysRevD.104.L111102](https://doi.org/10.1103/PhysRevD.104.L111102)

I. INTRODUCTION

Gauge-singlet pseudoscalar particles have been attracting attention for many years in view of understanding the phenomenology of the strong CP problem (lack of CP violation in QCD) [1–3]. Such particles appear in models with a spontaneously broken global symmetry and are considered as candidates for either dark matter or for mediators to a dark sector (see e.g., Refs. [4–11]).

Previously, a neutral pseudoscalar particle a decaying to e^+e^- [12,13] was proposed to explain the ATOMKI anomaly [14–16]. Such particles could also cause a deviation from the expected value of the electron anomalous magnetic moment [17–19].

The NA64 experiment previously derived limits on light vector particles decaying to e^+e^- [20]. The production cross section and decay width of a pseudoscalar particle differ from the corresponding values predicted for a vector particle with the same mass. In this paper we use the available data of the NA64 experiment and some results of the previous analyses of these data to derive limits on the particle a .

II. THE SEARCH METHOD

The NA64 experiment in the “visible mode” configuration, i.e., configured for searches for dark matter particles, such as dark photons A' or a particles, decaying visibly, into e^+e^- pairs, is described in Refs. [20,21] and shown in Fig. 1.

The experiment uses the high purity H4 electron beam at the CERN SPS (beam energy 100 GeV in 2017 and 150 GeV in 2018). The backgrounds coming from the beam are further significantly suppressed by using the

synchrotron radiation detector (SRD) to identify electrons [22]. This suppression factor for the hadron contamination of the beam is $\sim 10^{-4}$. The most important subdetectors in this setup are the two electromagnetic (EM) calorimeters; the compact target-calorimeter WCAL assembled from the tungsten and plastic scintillator plates with wavelength shifting fiber read-out and ECAL, a matrix of 6×6 shashlik-type lead-plastic scintillator sandwich modules [22]. We also use a veto counter W_2 placed immediately after the WCAL and a decay counter S_4 installed downstream the vacuum decay tube. Measuring the energy deposition in W_2 ensures that no charged particle exits from the WCAL, while a signal compatible with two minimum ionizing particles (MIPs) in S_4 indicates that a decay to e^+e^- happened in the decay volume. The high efficiency thick (5 cm) counter VETO and the hadron calorimeter HCAL are installed downstream the ECAL. The HCAL consists of four modules—three of them are placed at the axis of the beam deflected by the MBPL magnets. They are usually used as a veto against electroproduction of hadrons in the WCAL. The fourth module serves as a veto against upstream interactions of electrons before reaching the target. Some most important distances of the setup are shown in Table I. The distances in the invisible mode configuration in 2016 and 2017 were slightly different; this was taken into account in the exact signal yield calculation, which can be made only using the detailed simulation.

If the particle a exists, it would be produced via scattering of high-energy electrons off nuclei of an active target-dump WCAL due to its coupling to electrons $e\bar{e}$,

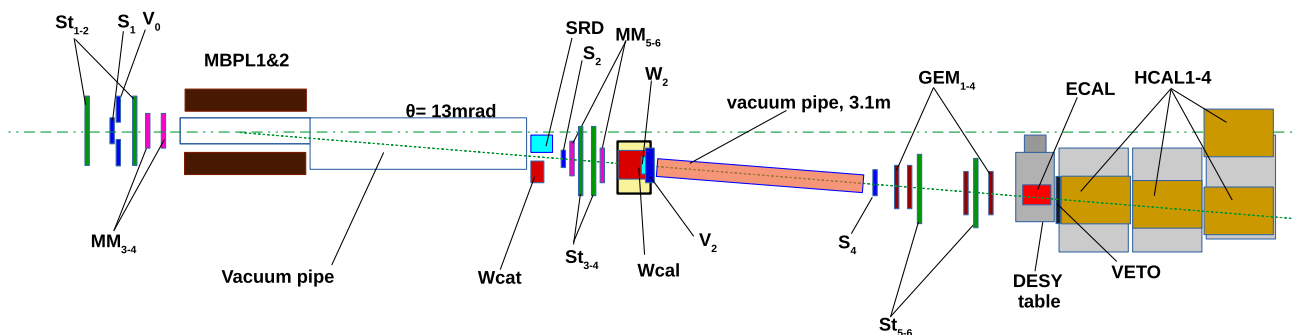


FIG. 1. The NA64 setup to search for $A'(a) \rightarrow e^+e^-$ decays of the bremsstrahlung $A'(a)$ produced in the reaction $eZ \rightarrow eZA'(a)$ of the 150 GeV electrons incident on the active WCAL target. The figure is reproduced from Ref. [20].

TABLE I. Some parameters and distances of the NA64 experimental setups.

Run	Beam energy (GeV)	Calorimeter size along the beam (cm)	Distance end of calorimeter–end of veto (cm)	Decay length (m)
2017 visible mode	100	17.3	2.7	3.12
2018 visible mode	150	17.3	0.6	3.14
2018 invisible mode geom.	100	45	198	$\simeq 3.4$

where e is the electron charge and ϵ is a coupling parameter [23]. The Lagrangian term corresponding to the coupling with electrons ψ_e is $\mathcal{L} \supset -i\epsilon e a \bar{\psi}_e \gamma_5 \psi_e$. The a production is followed by its decay into e^+e^- pairs,

$$e^- + Z \rightarrow e^- + Z + a; a \rightarrow e^+e^-. \quad (1)$$

The a can be detected if it decays in flight beyond the rest of the dump and the veto counter W_2 in the decay volume. The occurrence of the process (1) would manifest itself as an excess of events with two EM-like showers in the setup, one in the WCAL and another one in the ECAL, with the total energy $E_{\text{tot}} = E_{\text{WCAL}} + E_{\text{ECAL}}$ compatible with the beam energy (E_0), above those expected from background sources. In the design of the “visible mode” setup we took into account that in a part of the parameter space to be explored the particle a is rather short-lived. The distance from the creation zone to the end of veto (W_2 counter) was minimized.

The candidate events are selected by applying the following main criteria:

- (1) The upper cut on the energy deposition in the W_2 veto counter is ~ 0.7 MIP (most probable energy deposition of a minimum ionizing particle), or 0.0007 GeV;
- (2) The lower cut on the signal in S_4 decay counter is 1.5 MIPs (0.0003 GeV);
- (3) $E_0 - E_{\text{tot}}$ is smaller than double total uncertainty of this difference; the energy in the downstream calorimeter $E_{\text{ECAL}} > 25$ GeV;
- (4) The shower in the WCAL must be consistent with that produced by a primary electron, we use a WCAL preshower lower-energy cut of 0.5 GeV to check this;
- (5) The cell with maximal energy deposition in the ECAL should be the one on the deflected beam axis;
- (6) The longitudinal and lateral profiles of the shower in the ECAL are consistent with a single EM shower. The longitudinal shape is checked by requiring an energy deposition of at least 3 GeV in the ECAL preshower. The lateral profile of the shower was compared to the profile measured in the calibration beam using the χ^2 method. This does not decrease the efficiency for signal events because the distance between e^- and e^+ in the ECAL is significantly smaller than the ECAL cell size of 3.82×3.83 cm²;

- (7) The rejection of events with hadrons in the final state is based on the energy deposition in the VETO counter (less than 0.9 MIP = 0.09 GeV required) and the hadron calorimeter HCAL (less than 1 GeV for each module required).

The cuts used for the event selection are explained in more detail in the previous paper [20].

In order to increase the sensitivity to a at small values of ϵ (below $\sim 2 \times 10^{-4}$), we also used the NA64 data collected in 2016–2018 in the “invisible mode” configuration [24] with only one electromagnetic calorimeter ECAL serving as a target, with an analysis scheme exactly as in our ALP search [25] (the picture of the setup can be found in the same reference). In this method the HCAL is used not only as a veto, but also as a detector of possible $a \rightarrow e^+e^-$ decays.

The “invisible mode” configurations are characterized by much longer distance from the creation zone to the end of veto, as can be seen in Table I. However, for small values of ϵ this is not a problem as the particle a is relatively long-lived. There is a significant probability that after its creation in the ECAL and passing the first HCAL1 module serving as a shield/veto it would be observed in the NA64 detector in one of the two signatures: (S1) as an event with $a \rightarrow e^+e^-$ decay inside the HCAL2 or HCAL3 modules (HCAL2,3 in the following), or (S2) as an event with a significant missing energy if it decays beyond HCAL2,3. In both cases the main requirements were that the shower profile in ECAL is compatible with electron, the VETO counter signal is smaller than 0.9 MIP and that the energy deposition in HCAL1 is smaller than 1 GeV. The main requirements for the signature (S1) event were that the total energy deposition in HCAL $E_{\text{HCAL}} \gtrsim 15$ GeV, and that the energy deposited in HCAL2,3 is concentrated in the central cell [25]. For the signature (S2) the total energy deposition in ECAL was required to be smaller than 50 GeV and the energy in all HCAL modules should be smaller than 1 GeV. There was also a number of other criteria explained in more details for the signature (S1) in [25] and for the signature (S2) in [22,24].

As the event selection was exactly the same as in the previous analyses, we reused the results of the background estimation from them. The main background in the NA64 “visible mode” configuration comes from the electroproduction of K_S^0 and their decays $K_S^0 \rightarrow \pi^0\pi^0$ in flight, followed by conversion of one of the decay photons.

TABLE II. Main data bins of the statistical analysis.

Data bin	1. Visible mode configuration	2. Invisible mode configuration, signature (S1)	3. Invisible mode configuration, signature (S2)
Total number of EOT	8.4×10^{10}	2.84×10^{11}	2.84×10^{11}
Background	0.083	0.1	0.472
Signal $m_a = 10$ MeV, $\epsilon = 10^{-4}$	1.32	6.7	1.4

After optimization of the setup in 2018 this background, determined from data, amounted to less than 0.005 events per 10^{10} EOT [20]. The main background in the “invisible mode” configuration comes from neutral hadron production by electrons in the target. These neutral hadrons either pass without interaction the first HCAL module and deposit energy in the downstream modules HCAL2,3, or completely escape detection because of insufficient aperture of the HCAL. These backgrounds, of the order of 0.1 events, were also determined from data [24,25].

III. SIGNAL YIELD AND RESULTS

In the calculations of the signal yield we used the fully GEANT4 [26] compatible package DMG4 [27]. This package can simulate the production of four types of DM mediator particles in the electron bremsstrahlung processes, including the vector and pseudoscalar cases. It contains a collection of corresponding cross sections, total and differential, including the ones for a pseudoscalar particle a from the model of Ref. [12]. The total cross sections are calculated at the exact tree level (ETL). We assumed that the a decay branching ratio to e^+e^- is 100%.

The package DMG4 was compiled together with the program based on Geant4 for the full simulation of the NA64 experimental setup. The produced signal samples were processed by the same reconstruction program as the real data and passed the same selection criteria.

We remind that no candidate events were found in all previously made analyses that we reuse and combine here. For the statistical analysis, there were three main data bins, see Table II. The bins 1 and 3 were further subdivided into bins corresponding to different years and conditions. The total number of bins was up to 9. The backgrounds and various uncertainties in these bins were estimated in the previously published analyses [20,22,24,25] and reused. This concerns also most of the signal yield uncertainties. The uncertainties depending on the a energy and path to decay distributions were recalculated for the new signal samples, but turned out to be compatible with the values determined previously and remained unchanged. All uncertainties, summed up in quadrature, don’t exceed 20%.

The exclusion limits were calculated by employing the multi-bin limit setting technique in a program based on RooStats package [28] with the modified frequentist approach, using the profile likelihood as a test statistic

[29–31]. The 90% C.L. excluded region in the two-dimensional plot $m_a - \epsilon$ is shown in Fig. 2. The regions excluded by the $(g-2)_e$ measurements are also shown, the most stringent is LKB [18]. The central value of this measurement has the sign opposite to possible contribution from a pseudoscalar particle a coupled to electrons. We used a frequentist approach to calculate the 90% C.L. limit from it. We note that the limits from the $(g-2)_e$ measurements are model dependent and can be significantly less strict in some scenarios [11,32].

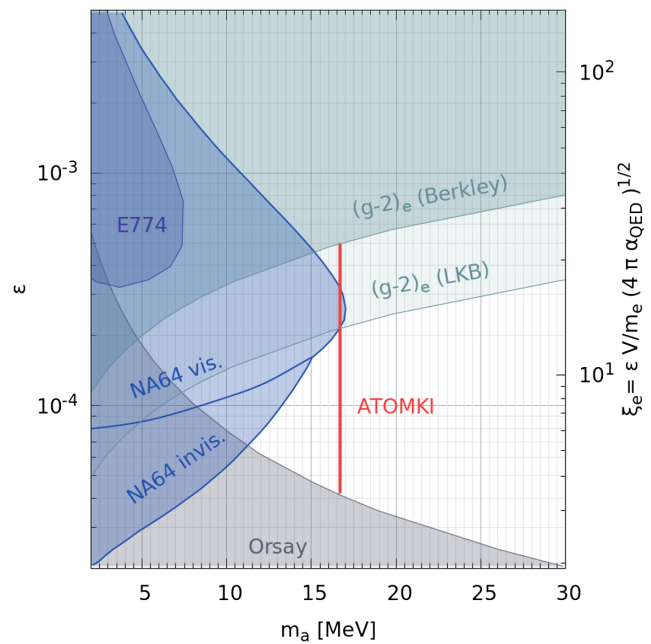


FIG. 2. The 90% C.L. limits on the pseudoscalar particles decaying to e^+e^- pairs. On the right vertical axis we use the standard notation for the pseudoscalar coupling $\xi_e = \epsilon(V/m_e)\sqrt{4\pi\alpha_{\text{QED}}}$, where $V = 246$ GeV is a vacuum expectation value of the Higgs field [33]. This corresponds to the Lagrangian term $\mathcal{L} \supset -i\xi_e \frac{m_e}{V} a\bar{\psi}_e\gamma_5\psi_e$. The red vertical line corresponds to the ATOMKI anomaly at $m_a = 16.7$ MeV (central value of the first result on beryllium). The ϵ range excluded at this mass is $2.1 \times 10^{-4} < \epsilon < 3.2 \times 10^{-4}$. The region excluded using only the data collected with the visible mode geometry is denoted as “NA64 vis.,” the extension of this region obtained using all data is denoted as “NA64 invis.,” The regions excluded by the $(g-2)_e$ measurements (Berkeley [17] and LKB [18]) are shown. The limits from the electron beam-dump experiments E774 [34] and Orsay [35] are taken from Ref. [33].

IV. CONCLUSION

We performed a model-independent search for light pseudoscalar particles that couple to electrons and decay predominantly to e^+e^- pairs in the NA64 experiment at the CERN SPS North Area. The active target calorimeter of this experiment was exposed to the electron beams with the energy of 100 and 150 GeV. No signal of such particles was found, allowing us to exclude the region of the (m_a, ϵ) parameter space in the mass range from 1 to 17.1 MeV. Additional exposure will increase sensitivity, in particular at the mass of the ATOMKI anomaly of 16.7 MeV [36].

ACKNOWLEDGMENTS

We gratefully acknowledge the support of the CERN management and staff and the technical staff of the participating institutions for their vital contributions.

We thank Robert Ziegler for useful comments about the a contribution to $(g-2)_e$. This work was supported by the Helmholtz-Institut für Strahlen- und Kernphysik (HISKP), University of Bonn, the Carl Zeiss Foundation 0653-2.8/581/2, and Verbundprojekt-05A17VTA-CRESST-XENON (Germany), Joint Institute for Nuclear Research (JINR) (Dubna), the Ministry of Science and Higher Education (MSHE) and RAS (Russia), ETH Zurich and SNSF Grants No. 169133, No. 186181, and No. 186158 (Switzerland), Tomsk Polytechnic University, FONDECYT Grants No. 1191103, No. 190845, and No. 3170852, UTFSM PI M 18 13, ANID PIA/APOYO AFB180002 (Chile) and Millennium Institute for Subatomic Physics at the High-Energy Frontier (SAPHIR) of ANID, Code: ICN2019_044. The work on the DMG4 package was supported by the Russian Science Foundation RSF Grant No. 21-12-00379.

-
- [1] R. D. Peccei and H. R. Quinn, *Phys. Rev. Lett.* **38**, 1440 (1977).
- [2] S. Weinberg, *Phys. Rev. Lett.* **40**, 223 (1978).
- [3] F. Wilczek, *Phys. Rev. Lett.* **40**, 279 (1978).
- [4] R. Essig *et al.*, arXiv:1311.0029.
- [5] J. Alexander *et al.*, arXiv:1608.08632.
- [6] M. Battaglieri *et al.*, arXiv:1707.04591.
- [7] J. Beacham *et al.*, *J. Phys. G* **47**, 010501 (2020).
- [8] R. K. Ellis *et al.*, arXiv:1910.11775.
- [9] A. Berlin, N. Blinov, G. Krnjaic, P. Schuster, and N. Toro, *Phys. Rev. D* **99**, 075001 (2019).
- [10] E. Aprile *et al.*, *Phys. Rev. D* **102**, 072004 (2020).
- [11] D. Buttazzo, P. Panci, D. Teresi, and R. Ziegler, *Phys. Lett. B* **817**, 136310 (2021).
- [12] D. S. Alves, *Phys. Rev. D* **103**, 055018 (2021).
- [13] U. Ellwanger and S. Moretti, *J. High Energy Phys.* **11** (2016) 039.
- [14] A. J. Krasznahorkay *et al.*, *Phys. Rev. Lett.* **116**, 042501 (2016).
- [15] A. Krasznahorkay *et al.*, arXiv:1910.10459.
- [16] A. J. Krasznahorkay, M. Csatlós, L. Csige, J. Gulyás, A. Krasznahorkay, B. M. Nyakó, I. Rajta, J. Timár, I. Vajda, and N. J. Sas, *Phys. Rev. C* **104**, 044003 (2021).
- [17] R. H. Parker, C. Yu, W. Zhong, B. Estey, and H. Müller, *Science* **360**, 191 (2018).
- [18] L. Morel, Z. Yao, P. Cladé, and S. Guellati-Khélifa, *Nature (London)* **588**, 61 (2020).
- [19] Y. M. Andreev *et al.*, *Phys. Rev. Lett.* **126**, 211802 (2021).
- [20] D. Banerjee *et al.*, *Phys. Rev. D* **101**, 071101 (2020).
- [21] D. Banerjee *et al.*, *Phys. Rev. Lett.* **120**, 231802 (2018).
- [22] D. Banerjee *et al.*, *Phys. Rev. D* **97**, 072002 (2018).
- [23] Y.-S. Liu and G. A. Miller, *Phys. Rev. D* **96**, 016004 (2017).
- [24] D. Banerjee *et al.*, *Phys. Rev. Lett.* **123**, 121801 (2019).
- [25] D. Banerjee *et al.*, *Phys. Rev. Lett.* **125**, 081801 (2020).
- [26] S. Agostinelli *et al.*, *Nucl. Instrum. Methods Phys. Res., Sect. A* **506**, 250 (2003).
- [27] M. Bondi, A. Celentano, R. R. Dusaev, D. V. Kirpichnikov, M. M. Kirsanov, N. V. Krasnikov, L. Marsicano, and D. Shchukin, *Comput. Phys. Commun.* **269**, 108129 (2021).
- [28] I. Antcheva *et al.*, *Comput. Phys. Commun.* **182**, 1384 (2011).
- [29] T. Junk, *Nucl. Instrum. Methods Phys. Res., Sect. A* **434**, 435 (1999).
- [30] G. Cowan, K. Cranmer, E. Gross, and O. Vitells, *Eur. Phys. J. C* **71**, 1554 (2011).
- [31] A. L. Read, *J. Phys. G* **28**, 2693 (2002).
- [32] D. S. M. Alves and N. Weiner, *J. High Energy Phys.* **07** (2018) 092.
- [33] S. Andreas, O. Lebedev, S. Ramos-Sánchez, and A. Ringwald, *J. High Energy Phys.* **08** (2010) 003.
- [34] A. Bross, M. Crisler, S. Pordes, J. Volk, S. Errede, and J. Wrbanek, *Phys. Rev. Lett.* **67**, 2942 (1991).
- [35] M. Davier and H. N. Ngoc, *Phys. Lett. B* **229**, 150 (1989).
- [36] E. Depero *et al.*, *Eur. Phys. J. C* **80**, 1159 (2020).